

DOCUMENT CONTROL DATA - R & D

(Security classification of title, body of abstract and indexing annotation must be entered when the overall report is classified)

1. ORIGINATING ACTIVITY (Corporate author) Naval Research Laboratory Washington, D. C. 20390		2a. REPORT SECURITY CLASSIFICATION Unclassified	
		2b. GROUP	
3. REPORT TITLE KINETICS OF THE CHLORIDE-INDUCED OXIDATION OF IRON AT 300°C			
4. DESCRIPTIVE NOTES (Type of report and inclusive dates) An interim report on a continuing NRL problem.			
5. AUTHOR(S) (First name, middle initial, last name) M. A. Scheiman			
6. REPORT DATE February 8, 1971		7a. TOTAL NO. OF PAGES 22	7b. NO. OF REFS 27
8a. CONTRACT OR GRANT NO. NRL Problem C05-29		9a. ORIGINATOR'S REPORT NUMBER(S) NRL Report 7204	
b. PROJECT NO. RR 007-02-41-5678			
c.		9b. OTHER REPORT NO(S) (Any other numbers that may be assigned this report)	
d.			
10. DISTRIBUTION STATEMENT Approved for public release; distribution unlimited.			
11. SUPPLEMENTARY NOTES		12. SPONSORING MILITARY ACTIVITY Department of the Navy (Office of Naval Research), Arlington, Va. 22217	
13. ABSTRACT Iron was oxidized in the absence of oxygen at 300°C in solutions containing chloride and/or iron(II) ions. The oxidation reaction $3\text{Fe} + 4\text{H}_2\text{O} \rightarrow \text{Fe}_3\text{O}_4 + 4\text{H}_2 \quad \Delta G_{300^\circ\text{C}} = -10.3 \text{ kcal/mole Fe}_3\text{O}_5 \quad (1)$ was conveniently studied by the hydrogen-effusion method, which determines the rate at which hydrogen is evolved. The electrolytes in solution affect the reaction rate of Eq. (1) but, except for iron(II), do not enter into the final reaction products. The generally accepted concept that chloride ions accelerate the oxidation of iron has not received experimental verification, because, in addition to chloride ions, the system must contain iron(II) ions. An empirical equation has been derived that describes the extent of iron oxidation W with time t as a function of the iron(II) chloride molar concentrations; viz, $W = a \log (bt + 1) + k' [\text{Fe}^{2+}]^{1/2} [\text{Cl}^-]^{1/2} t, \quad (2)$ where a and b are adjustable parameters and k' is the kinetic rate constant for the steady-state condition of constant oxidation rate. The first term, or the log term, has been described as an oxidation mechanism in which an oxide film, containing pores that are			

(Continued on next page)

14. KEY WORDS	LINK A		LINK B		LINK C	
	ROLE	WT	ROLE	WT	ROLE	WT
Boiler corrosion Oxidation rates Mild Steel Chlorides Chloride-catalyzed oxidation of iron Reaction kinetics Oxidation Mechanism Heterogeneous phase observation Magnetite						

ABSTRACT (Continued)

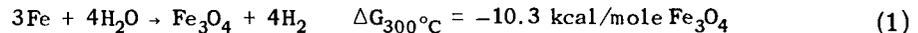
continuously being filled and regenerated, influences the reaction rate. Magnetite, or Fe_3O_4 , is deposited as a tightly adherend crystalline film at the metal/solution interface and apparently also quenches the reaction rate by serving as a physical barrier. The differential with respect to time of the second term of Eq. (2) describes a rate mechanism that is proceeding under the diffusive control of ions migrating across the Nernst boundary layers of anodic and cathodic regions of an oxide-free metal/solution interface.

CONTENTS

Abstract	ii
Problem Status	ii
Authorization	ii
INTRODUCTION	1
EXPERIMENTAL SECTION	1
Chemicals	1
Procedure	2
RESULTS	4
DISCUSSION	10
ACKNOWLEDGMENTS	16
REFERENCES	17

ABSTRACT

Iron was oxidized in the absence of oxygen at 300°C in solutions containing chloride and/or iron(II) ions. The oxidation reaction



was conveniently studied by the hydrogen-effusion method, which determines the rate at which hydrogen is evolved. The electrolytes in solution affect the reaction rate of Eq. (1) but, except for iron(II), do not enter into the final reaction products. The generally accepted concept that chloride ions accelerate the oxidation of iron has not received experimental verification, because, in addition to chloride ions, the system must contain iron(II) ions. An empirical equation has been derived that describes the extent of iron oxidation W with time t as a function of the iron(II) chloride molar concentrations; viz,

$$W = a \log (bt + 1) + k' [\text{Fe}^{2+}]^{1/2} [\text{Cl}^-]^{1/2} t, \quad (2)$$

where a and b are adjustable parameters and k' is the kinetic rate constant for the steady-state condition of constant oxidation rate. The first term, or the log term, has been described as an oxidation mechanism in which an oxide film, containing pores that are continuously being filled and regenerated, influences the reaction rate. Magnetite, or Fe_3O_4 , is deposited as a tightly adherent crystalline film at the metal/solution interface and apparently also quenches the reaction rate by serving as a physical barrier. The differential with respect to time of the second term of Eq. (2) describes a rate mechanism that is proceeding under the diffusive control of ions migrating across the Nernst boundary layers of anodic and cathodic regions of an oxide-free metal/solution interface.

PROBLEM STATUS

This an interim report on one phase of the problem; work is continuing.

AUTHORIZATION

NRL Problem C05-29
Project RR 007-02-41-5678

Manuscript submitted September 25, 1970.

KINETICS OF THE CHLORIDE-INDUCED OXIDATION OF IRON AT 300°C

INTRODUCTION

It has been generally considered that the chloride ion has the unique property to accelerate the oxidation of iron. A recent survey of the literature to 1968 (1,2) on the role of the chloride ion on the oxidation of iron has found no generally accepted explanation of the mechanism by means of which halide ions participate in the oxidation reaction other than that the halide ions are capable of being adsorbed at the iron/solution interface. There is also much conflicting experimental evidence on the role of the chloride ion in the oxidation reaction such as to lead to a lack of agreement on whether to classify chloride ions as oxidation promoters or retarders.

Iron, with a standard electrode potential of -0.440 volts, would be expected to be thermodynamically unstable with respect to oxygen and water. However, the thin continuous adherent film of the iron oxides that rapidly forms on nascent iron surfaces acts as a barrier between the metal and the oxidizing environment and effectively retards the rate of oxidation. The perfection and growth of such films by the action of high-temperature water and selected aqueous solutions have been used to explain the low rates of iron oxidation in steam boilers (3). Under ideal conditions, steam in such boilers is generated in the absence of gaseous oxygen. Slater and Parr (4) have discussed the conditions under which iron boiler walls have become pitted and eventually penetrated by chloride-ion-laden boiler waters. Potter and Mann (5) have reported that mild steel oxidizes rapidly above 200°C in dilute solutions of iron(II) chloride and that the oxidation products and the rates of reaction are typical of those found in on-load boilers. More recently, they report that solutions of sodium chloride have actually inhibited the oxidation rate of iron under the same conditions (6).

This investigation has been undertaken in an effort to resolve the conflicts posed by the previous investigators. Accordingly, the kinetics of the chloride-induced oxidation of iron at 300°C, in the absence of gaseous oxygen, has been studied in an attempt to elucidate the mechanism. The experimental parameters approximate those found in power-generating systems.

EXPERIMENTAL SECTION

Chemicals

The water used to prepare all the solutions was triply distilled, once from a Barnsted still and then through two stages of a quartz still. It was stored in tightly capped bottles of borosilicate glass. Hydrochloric acid, iron(II) chloride, and sulfuric acid were reagent-grade chemicals and used as received. The iron specimens were made from cold-drawn, low-carbon (0.9%) steel tubing which had a 0.634-cm O.D. and 0.051-cm walls. The analysis of these specimens is shown in Table 1. The inner and outer surfaces of the steel tubing were degreased and thoroughly abraded with fine steel wool after which the tubing was hydrogen annealed for 1 hour at 870°C. This procedure was followed by a 1-hour vacuum anneal at 870°C and a 16-hour slow cooling to room temperature in the furnace under vacuum.

Table 1
Analysis of the Iron Specimens

Constituent	Weight Percent
Carbon	0.09
Phosphorus	0.017
Sulfur	0.032
Nitrogen	0.007
Manganese	0.57
Silicon	0.07
Chromium	0.10
Nickel	0.07
Iron (by difference)	99.04

Procedure

The rate of iron oxidation as a function of time was measured by the hydrogen-effusion method, which has been previously described (7,8). This method uses the iron specimen in the form of a small metal capsule filled with 0.500 ± 0.003 g of solution. The capsule is maintained at a constant controlled temperature of 300°C in a vacuum oven. Under these conditions and in the absence of dissolved oxygen, iron oxidizes according to



At elevated temperatures, hydrogen gas diffuses or effuses easily through the iron wall of the capsule into the vacuum oven where the gas pressure is measured continuously as a function of time. The rate of hydrogen gas pressure change in the oven is used to determine the rate of iron oxidation according to

$$(\text{RATE}) = \frac{d(\text{Fe})}{dt} = 0.75 \frac{V}{ART} \left[\frac{\Delta P}{\Delta t} \right], \quad (2)$$

where

$\frac{d(\text{Fe})}{dt}$ = rate of iron oxidation at time t following the insertion of sample into into vacuum oven,

V = volume of the vacuum oven,

R = gas constant,

T = temperature of H_2 ,

A = measured geometrical surface area of the iron specimen in contact with the oxidizing electrolyte increased by 20% to allow for surface roughness (7),

$\frac{\Delta P}{\Delta t}$ = rate of hydrogen gas pressure change at time t following the insertion of the capsule into the vacuum oven.

Following the custom previously established in this laboratory, all iron oxidation rates are expressed in terms of milligrams of iron oxidized per square decimeter of geometrical surface in contact with the electrolyte per month; to convert this value to moles

of iron oxidized per square centimeter per minute, multiply by 4.4×10^{-12} . The range of hydrogen pressures measured rose from 0.1 to 50 microns Hg, after which the vacuum oven was evacuated and the cycle repeated.

The capsule systems, e.g., iron specimens containing an encapsulated solution, that were prepared to be studied at 300°C are given in Table 2. Several capsule systems burst within minutes following insertion into the high-temperature vacuum oven. When possible, these systems were replaced. Such failures were always due to imperfectly sealed ends. All of the capsules containing the 10^{-3} M and 5×10^{-4} M FeCl_2 and 10^{-1} M NaCl solutions were kept in the vacuum oven till failure occurred. Failure was signaled by the onset of a sudden and rapid pressure increase and/or by the appearance of an aqueous condensate in the cooler portions of the vacuum system. Following the corrosive penetration of the wall, the capsule was withdrawn from the furnace section of the vacuum system, cooled to room temperature, and removed from the vacuum system.

Table 2
Sets of Capsule Systems Prepared to be Studied at 300°C

Set	Encapsulated Solution	Conc. (moles/liter)	pH of Soln. before Encapsulation	Remarks
A	FeCl_2	1×10^{-3}	5.70	—
B	FeCl_2	5×10^{-4}	3.00	Capsule filled with 10^{-3} M HCl to generate FeCl_2 in situ
C	FeCl_2	5×10^{-5}	4.00	Capsule filled with 10^{-4} M HCl to generate FeCl_2 in situ
D	FeCl_2	1×10^{-3}	5.70	Inner walls of capsule washed twice with FeCl_2 soln. before final filling
E	NaCl	1×10^{-3}	6.15	—
F	NaCl	1×10^{-1}	5.92	—
G	FeSO_4	5×10^{-4}	3.00	Capsule filled with 5×10^{-4} M H_2SO_4 to generate FeSO_4 in situ
H	H_2O	-	5.80	Triply distilled

The pH of any solution recovered from a capsule was determined on a Beckman model GS pH meter equipped with a 289-82 microelectrode capable of measuring volumes on the order of 0.05 ml. The electrode system was protected by a nitrogen atmosphere, and the determination was made at 25°C.

Randomly selected FeCl_2 capsule systems were opened and drained of any remaining liquid. Capsules were sectioned by means of a jeweler's saw, washed in acetone, dehydrated, and stored in a vacuum desiccator. The opened capsules were examined visually and under high-powered microscopic magnification. The oxide/solution interface of a capsule system containing 5×10^{-4} M FeCl_2 was examined under an electron microscope. Sections of the oxide-coated inner walls were also subjected to x-ray diffraction analysis (9).

RESULTS

The kinetics of the oxidation of iron by the solution of electrolytes has been determined by measuring the rate of hydrogen gas evolution in accordance with Eqs. (1) and (2). The experimental results of the oxidation rates at 300°C as a function of time are given in Figs. 1, 2, 3, and 4. Each curve in Figs. 2, 3, and 4 represents the averaged results of the duplicate runs of any particular set. The number of duplicate runs per set is given in Table 3. The pH of the solutions recovered from the various capsule systems averaged 6.9. In the case of the capsule system that had been originally filled with 10^{-4} M HCl (pH 4.00) (Set C), this averaged pH represents a reduction of 99.9% of the hydrogen ion activity or 10^{-4} M of chloride ions that presumably are not balanced electrically by an equivalent of counterions. To satisfy the conditions of electroneutrality, an equivalent quantity of the metal substrate is assumed to have entered into solution as hydrated ions.

The progress of the experimental oxidation process may be obtained from Fig. 1, which is typical of all the systems investigated. At zero time the capsule system, which is at 25°C, is inserted into the vacuum oven maintained at 300°C. Depending on the conditions, it will take the capsule 24 to 29 minutes to reach the temperature of the oven; meanwhile, the oxidation rate is increasing with the temperature. In all the capsule systems investigated, the logarithm of the oxidation rate increased linearly with time. After the maximum oxidation rate, hereafter termed the peak oxidation rate, is reached, the reaction rate decreased at a rate, depending on the nature and concentration of the added electrolyte, to a steady-state condition of constant oxidation rate, hereafter termed the plateau oxidation rate. Table 3 contains the mean peak and plateau oxidation rates for sets A to H.

The sets A, B, C, and D containing iron(II) chloride, Figs. 2 and 3, developed extraordinarily large peak and plateau region oxidation rates when compared to distilled water (set H), Fig. 4. In Fig. 2, the peak rate of 10^{-3} M FeCl_2 (set A) is 2.27×10^5 , which is beyond the scale of the graph, and 5×10^{-5} M FeCl_2 (set C) did not reach the

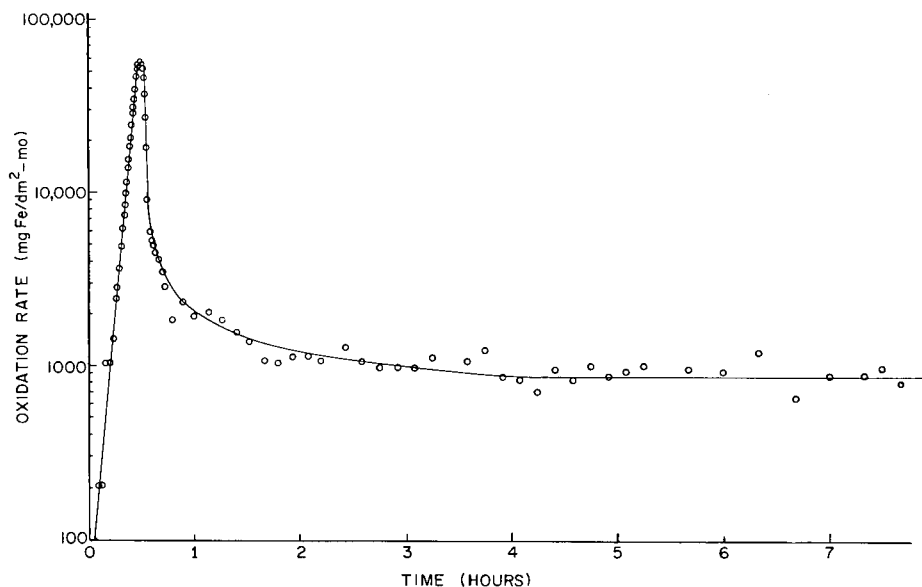


Fig. 1 - Oxidation rate of iron as a function of time for a sample system containing 5×10^{-4} M iron(II) chloride

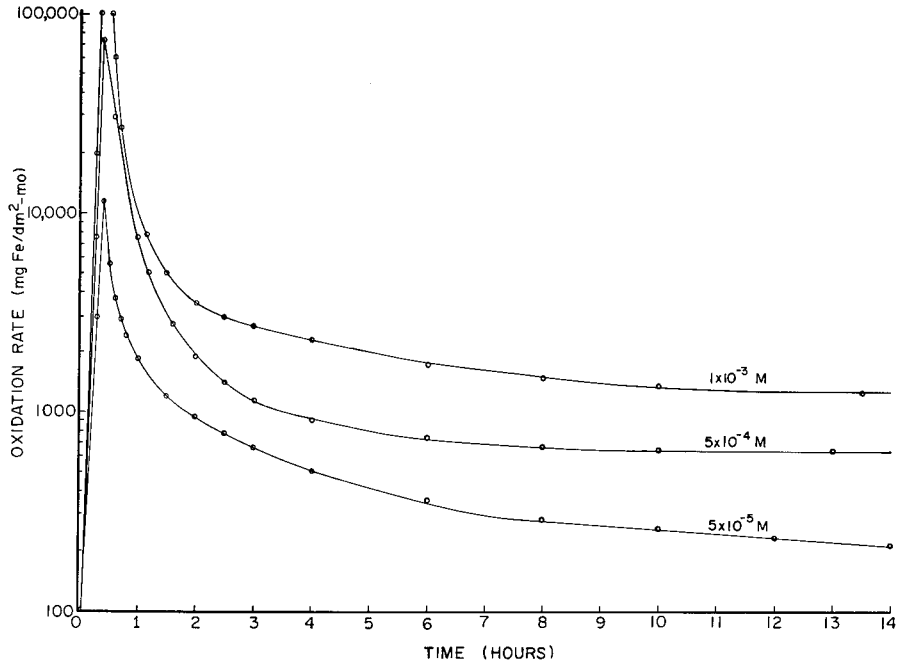


Fig. 2 - Oxidation rate of iron for sets A ($1 \times 10^{-3}M$ FeCl₂), B ($5 \times 10^{-4}M$ FeCl₂), and C ($5 \times 10^{-5}M$ FeCl₂) as a function of time

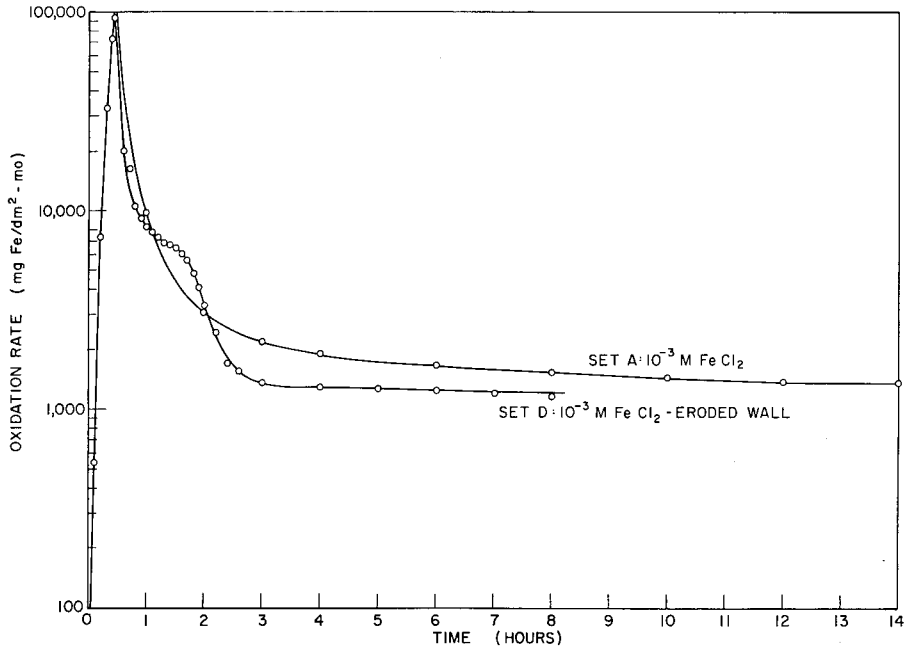


Fig. 3 - Oxidation rate of iron for sets A ($1 \times 10^{-3}M$ FeCl₂) and D ($1 \times 10^{-3}M$ FeCl₂, surface eroded with Fe(II)) as a function of time

Table 3
Mean Oxidation Rates, Duration of Tests, and Total Iron Oxidized at 300°C

Set	No. Tested	Oxidation Rates (mg Fe/dm ² -mo)		Mean Duration of Test	Total Iron Oxidized (mg Fe/dm ²)	
		Peak x 10 ⁵	Plateau x 10 ³		At 10 hr	At end of test
A, (10 ⁻³ M FeCl ₂)	4	2.27 ± 0.25	1.38 ± 0.10	11.9 ± 6.5 hr*	75.92 ± 9.67	112.1 ± 24.9
B, (5 x 10 ⁻⁴ M FeCl ₂)	4	0.76 ± 0.09	0.730 ± 0.097	12.1 ± 2.3 hr*	33.28 ± 3.22	36.37 ± 5.36
C, (5 x 10 ⁻⁵ M FeCl ₂)	2	0.12 ± 0.0	0.076 ± 0.012	70 days	9.83 ± 0.69	36.56 ± 5.20 [†]
D, (10 ⁻³ M FeCl ₂)	3	0.960 ± 0.073	1.17 ± 0.24	9.61 ± 0.56 hr*	47.12 ± 4.92 [‡]	45.74 ± 4.92
E, (10 ⁻³ M NaCl)	2	0.143 ± 0.003	0.032 ± 0.002	6 days	N.D.	N.D.
F, (10 ⁻¹ M NaCl)	2	0.117 ± 0.003	¶	40.5 hr*	N.D.	N.D.
G, (5 x 10 ⁻⁴ M FeSO ₄)	1	0.52	0.030	10 days	N.D.	N.D.
H, (H ₂ O, distilled)	1	0.0105	0.010	4 months	N.D.	N.D.

* Failed due to stress-corrosion cracking in the region of the welded ends.

[†] Calculated for 7-day period only. It is estimated that at the end of 70 days, the total iron oxidized was 177 mg Fe/dm².

[‡] Estimated.

N. D. Not determined.

¶ Failed before plateau region was reached. At the time of failure, oxidation rate was 96 ± 31 mg Fe/dm²-mo.

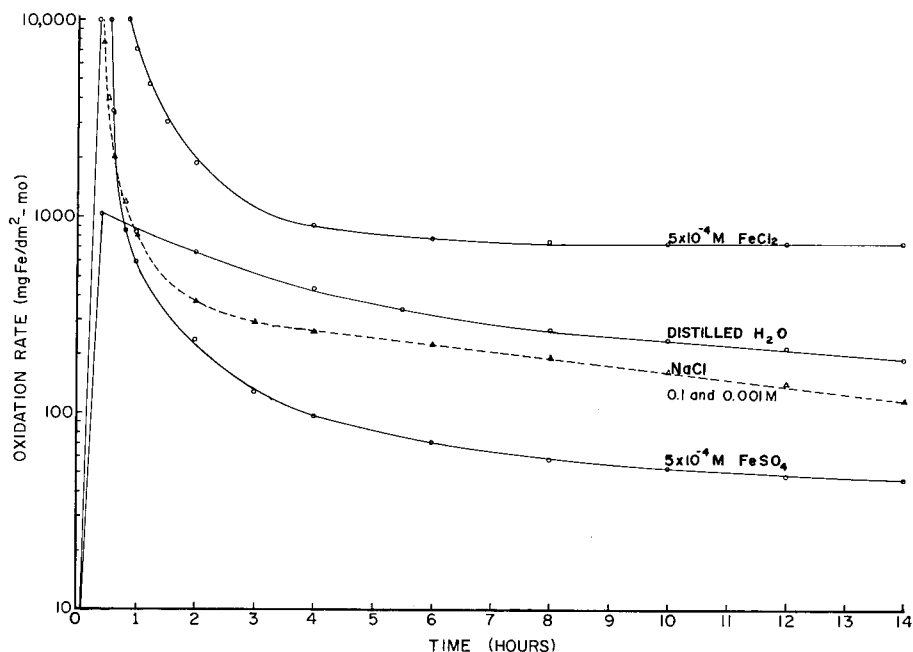


Fig. 4 - Oxidation rate for iron for sets B (5×10^{-4} M FeCl_2), E (1×10^{-3} M NaCl), F (1×10^{-1} M NaCl), G (5×10^{-4} M FeSO_4), and H (Distilled H_2O) as a function of time

plateau region oxidation rates until after 7 days. From the experimental data in Table 3, it was found that the oxidation rate for both the peak and the plateau regions could be expressed as functions of a kinetic rate constant and the electrolyte concentrations according to

$$(\text{RATE}) = \frac{dW}{dt} = k [\text{Fe}^{2+}]^{1/2} [\text{Cl}^-]^{1/2} \quad (3)$$

where W represents the weight of elemental iron being oxidized per square decimeter of geometrical surface, k is the kinetic rate constant, t represents time in months, and the bracketed ions are their respective concentrations in moles per liter in the solution at the start of the experiment. The value for the kinetic constant for the peak oxidation rate k_{peak} for sets A, B, and C is

$$k_{\text{peak}} = (1.46 \pm 0.26) \times 10^8 \frac{\text{mg Fe}}{\text{dm}^2\text{-mo}} \frac{1}{\text{mole}}, \quad (4)$$

while that for the plateau region of constant oxidation rate of sets A, B, C, and D is

$$k_{\text{plateau}} = (9.79 \pm 0.74) \times 10^5 \frac{\text{mg Fe}}{\text{dm}^2\text{-mo}} \frac{1}{\text{mole}}. \quad (5)$$

The percentage mean deviation for the peak oxidation rate constant is $\pm 18\%$ and that for the plateau region kinetic rate constant is $\pm 8\%$.

The comparative oxidative behavior at 300°C between sets A and D is given in Fig. 3. The average peak oxidation rate has been reduced from the previous high of 2.27×10^5 for the set A system to 9.60×10^4 mg Fe/dm²-mo for the D system. At 1.4 hours

there is evidence of the peak of a secondary oxidation rate process superimposed on the average oxidation rate-versus-time curve for the D system. At this point, the comparative average oxidation rates for sets A and D are 5.4×10^3 and 6.2×10^3 mg Fe/dm²-mo, respectively. The D system attained the plateau region oxidation rate at the end of 3 hours compared to the 11 hours necessary for the A system. The mean of the plateau region oxidation rates for the two curves in Fig. 3 is 1.28×10^3 mg Fe/dm²-mo. Their mean deviation of 9% is well within the experimental error.

The experimental values of dW/dt for sets A, B, C, and D were integrated to yield a curve of W , the quantity of iron oxidized per unit area, as a function of time t ; e.g.,

$$\int_0^t \left(\frac{dW}{dt} \right) dt = W \cdot f(t). \quad (6)$$

Mathematical analysis of this curve resulted in

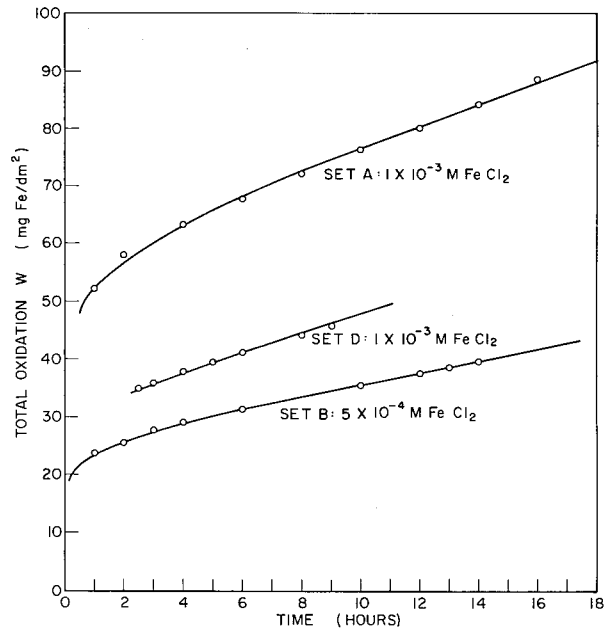
$$W = a \log (bt + 1) + k' [\text{Fe}^{2+}]^{1/2} [\text{Cl}^-]^{1/2} t. \quad (7)$$

The constants a and b are adjustable parameters that depend on the previous history of the capsule system, and k' is a kinetic rate constant that is identical to k_{plateau} used in Eq. (3). The values of the parameters a , b , and k' are given in Table 4. Figure 5 shows the experimental points of W as a function of t and the values calculated by Eq. (7) (the solid-line curve). There appears to be a remarkably good fit between the experiment and the derived equation in Fig. 5. Equation (7) indicates that at least two simultaneous rate mechanisms are in operation.

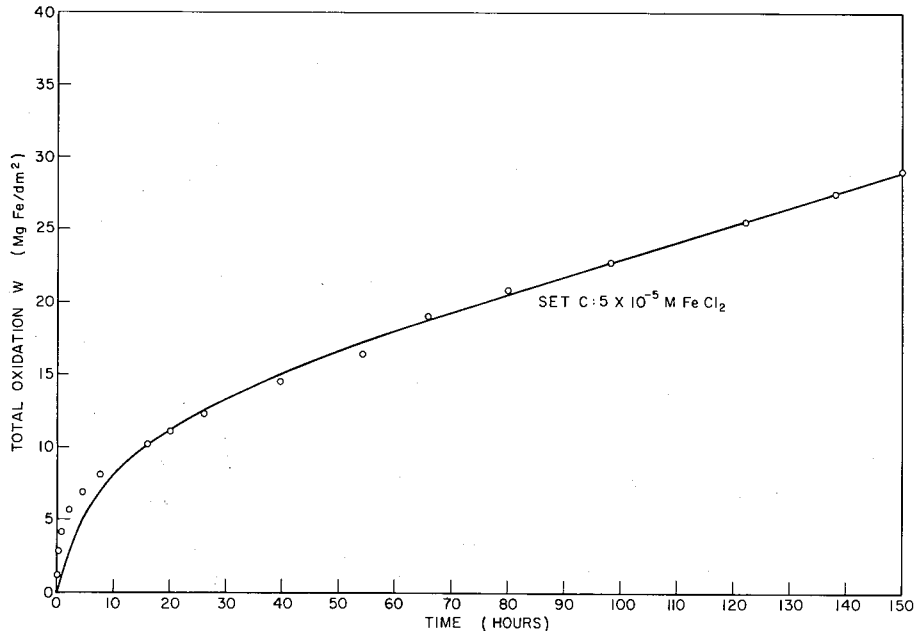
In Fig. 4 the oxidation behavior of systems containing 10^{-3}M and 10^{-1}M solutions of chloride ion as NaCl (sets E and F, respectively) and a system containing a $5 \times 10^{-4}\text{M}$ solution of iron(II) ions as FeSO₄ (set G) are compared with set H containing distilled water and set B containing stoichiometrically $5 \times 10^{-4}\text{M}$ iron(II) and 10^{-3}M chloride ions. The peak reaction rate for sets B and G are beyond the range of this graph and are given in Table 3. The E and F systems (10^{-3}M and 10^{-1}M NaCl, respectively) showed almost identical oxidative behavior and are represented for convenience by a single curve. However, the F system (10^{-1}M NaCl) failed before attaining the plateau region of the curve, which took 3 days for the set E system. The FeCl₂ system (set B) attained the plateau region after 9 hours of oxidation, the FeSO₄ system (set G) required 3 days, and the distilled water (set H) needed 90 days of oxidation to achieve the plateau region oxidation rates.

To avoid the introduction of additional variables, such as the accumulation of impurities or changes in the physical morphologies of the solid states, that would result from extended oxidations in the type of closed systems used in the current series of experiments, the time-rate data of the various reactions were not accumulated beyond the point necessary to establish the plateau regions.

The capsule systems, when sectioned, possessed a black adherent oxide phase on the iron substrate that was in contact with the solution. X-ray diffraction analysis indicated that Fe₃O₄, or magnetite, is the major surface phase (9), a result that is in accord with Eq. (1). An electron photomicrograph of the oxide/solution interface, Fig. 6, reveals well-formed crystallites of Fe₃O₄ that are epitaxially oriented with the separate grains of the underlying substrate (10). The well-formed crystal planes at the oxide/solution interface probably indicate crystal growth by deposition of ions from solution at elevated temperature.



(a)



(b)

Fig. 5 - Total oxidation of iron, W, as a function of time for sets A, B, C, and D. The curve is the locus of the equation $W = a \log(bt+1) + k' [\text{Fe}^{++}]^{1/2} [\text{Cl}^-]^{1/2} t$.

Table 4
Numerical Values for a, b, and k' of Eq. (7)

Set	FeCl ₂ Conc (mole/liter)	a (mg Fe/dm ²)	b (mg Fe/dm ² -mo)	$k' \times 10^5 \left(\frac{\text{mg Fe}}{\text{dm}^2\text{-mo}} \cdot \frac{1}{\text{mole}} \right)$
A	1×10^{-3}	10.43	5.11×10^7	8.14 ± 0.27
B	5×10^{-4}	5.11	1.76×10^5	8.14 ± 0.27
C	5×10^{-5}	7.47	6.48×10^2	8.14 ± 0.27
D	1×10^{-3}	2.45	2.38×10^{14}	8.14 ± 0.27

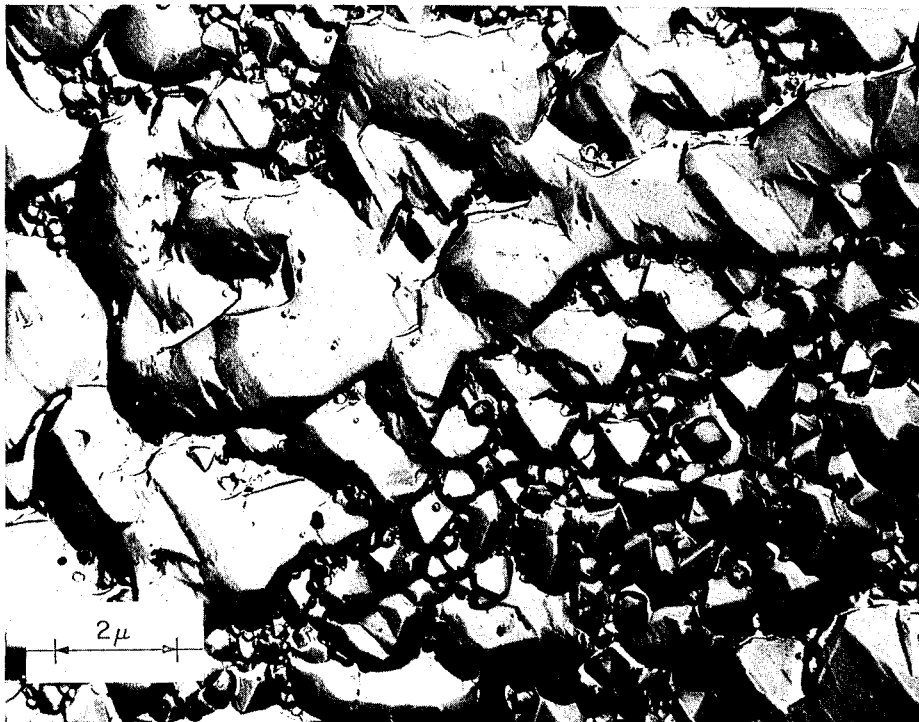


Fig. 6 - Electron photomicrograph of Fe₃O₄/solution interface of a set B (5×10^{-4} M FeCl₂) system whose wall ruptured at 300°C while undergoing oxidation in a vacuum oven

DISCUSSION

The A and D systems had been originally filled with iron (II) chloride solution, while sets B and C were filled with hydrochloric acid to form iron(II) chloride, in situ, by eroding the inner wall of the capsule. The encapsulated solutions of sets B and C presumably contain several of the soluble impurities of the substrate metal. However, Eq. (3) describes an oxidation rate (an exception is the peak rate of set D, which is a special case) that is solely the function of an electrolyte concentration which is assumed

to be constant with time in a given system, although the exact distribution of the constituent ions within the system presently remains unknown.

A comparison of the peak and plateau region oxidation rates for the B, E, F, G, and H systems in Table 3 along with their respective curves in Fig. 4 shows that both iron (II) and chloride ions must be simultaneously present, as suggested by Eq. (3), in order to achieve the high rates of iron oxidation formerly attributed to the sole effects of the chloride ion. However, the anomaly of an increased iron oxidation rate with an increased iron(II) concentration (in sets A, B, and C) must be considered. In the absence of a surface oxide film, the Nernst equation for the iron electrode contacting increasing concentrations of iron(II) chloride would predict a diminished potential for elemental iron to enter into solution as the solvated iron(II) ion, whereas Eq. (3) predicts an oxidation rate that is a direct function of the concentration of the electrolyte. In the presence of an oxide film at the metal/solution interface, the mechanism becomes the iron(II) chloride-induced oxidation of iron.

The first or log term on the right of Eq. (7) has been derived by Evans (11) and discussed by Harrison (12) as describing a mechanism of oxide film growth in which the oxide contains pores that are continuously being filled and regenerated. The second term on the right-hand side of Eq. (7) is the product of the plateau region oxidation rate equation that has been described in Eq. (3) and the time. In this case, it has reappeared as a result of the mathematical analysis of Eq. (6). The numerical value for k_{plateau} for Eq. (3) given in Eq. (5), is larger than that for k' for Eq. (7), given in Table 4. The former value had been originally obtained by dividing the iron(II) chloride concentration terms into a plateau region oxidation rate that contained elements of the logarithmic-term oxide film growth process. This condition is also reflected in the average mean deviation for k_{plateau} and k' of 8% and 3%, respectively.

The first term of Eq. (7), which suggests an oxide film growth proceeding by a pore filling-pore generating mechanism, is the major term numerically at small values of t ; it describes the region, in Figs. 1, 2, and 3, where the oxidation rate decreases from the peak rate to the plateau region where the reaction rate is determined solely by the electrolyte concentration according to Eq. (3). The second or linear term of Eq. (7) is the major term numerically at larger values of t ; it describes the plateau region where the oxidation rate is relatively constant with time. However, the plateau region still represents the sum of the elements of at least two rate processes expressed mathematically by a monotonically decreasing function with time that approaches asymptotically a second function that is constant with time. It would be reasonable to postulate that the experimental points about the curve in Fig. 1 that becomes the plateau region oxidation rate represent a dynamic equilibrium involving a cyclic mechanism of pore formation and pore closure (13).

The kinetic rate equation for the plateau region (Eq. (3)), the product of a kinetic rate constant and postulated constant electrolyte concentration terms, is a constant. Integration of this equation according to

$$\int_0^W dw = \int_0^t k_{\text{plateau}} [\text{Fe}^{2+}]^{1/2} [\text{Cl}^-]^{1/2} dt \quad (8)$$

yields

$$W = k_{\text{plateau}} [\text{Fe}^{2+}]^{1/2} [\text{Cl}^-]^{1/2} t, \quad (9)$$

which is identical to the linear term of Eq. (7). According to Evans (14) and Tomashov (15), Eq. (9) conforms to a linear law of oxide film growth. Films that grow according

to this linear law do not display a dependence of the oxidation rate on the thickness of the oxide film; they are considered to be nonprotective, and the oxidation process is controlled by the chemical reaction.

However, some systems display experimental kinetic oxidation rate constants that are much smaller than would be expected from a similar constant obtained from the reaction of a truly nonprotective film or an unobstructed surface (15). For these cases, the mechanism of film growth proceeds by the initial formation of a pseudomorphous oxide film that is a crystallographic continuation of the metal lattice. Since this film does not possess the true parameters of the oxide lattice, it displays no sign of stress. Films with thicknesses of one to two parameter units are rapidly formed when nascent iron surfaces are exposed to oxygen even at ambient temperatures (16). Continued oxidation increases the thickness of this layer until it reaches a critical size and is converted into the normal oxide with its own inherent lattice parameters and density. Internal stresses that now appear cause the outwardly growing oxide surface to fracture without affecting the thin continuous inner layer. The thickness of this inner layer, under conditions of constant temperature and electrolyte concentrations, remains approximately constant so that an oxidation rate under the control of the diffusion path through this layer remains constant.

In the present investigation, the values of k_{peak} (Eq. (4)) and k_{plateau} (Eq. (5)) are separated by approximately two orders of magnitude. While the hypothesis of a constant-thickness inner layer is reasonable, it must also account for the disparity in oxidation rates found between the systems that contained both iron(II) and chloride ions and those that contained them separately. Also, the crystal lattice of Fe_3O_4 displays orientational correspondence with the lattice of the α -iron substrate (17); e.g., the oxide lattice parameters are an extension of that of the substrate, so that there is a minimum displacement of the ions from their true parameters, and a pseudomorphous inner oxide is not required for the transition of the metal to the oxide phase.

In Fig. 6 the crystallites of Fe_3O_4 are epitaxially oriented with the lattice of the underlying substrate (10). Such films retard oxidation by simply reducing the metal solution interfacial area (18). Furthermore, the location and the nature of the oxide film porosity remain unresolved. However, Douglass (13) has attributed porosity in the region of the Fe_3O_4 /iron interface to vacancies caused by the depletion of iron at the metal oxidation zone. The coalescence of the vacancies into cavities coupled with the nonplasticity of Fe_3O_4 creates porous zones at the interface that periodically fill up and reopen. The high oxidation rates and linear law of film growth, Eq. (9), preclude the diffusion of ions through the lattice of the solid-state oxides. Oxide films generated in a manner similar to those formed in this investigation have had a high degree of porosity attributed to them (5, 10, 20). Bloom et al. (21) reported that the early stages of the oxidation by 15% NaOH proceeded by a pore-blocking mechanism and derived a log term for W similar to that in Eq. (7).

No direct relation exists between the quantity of oxide film reaction product that is deposited at the metal/solution interface at the peak and plateau regions and the reaction rates predicted by Eq. (3). It can be seen from Table 3 that the quantity of oxide film deposited at the interface is a variable quantity for these regions. Furthermore, the plateau region of constant oxidation rate retains its steady-state condition with time despite the continued formation of oxide film reaction product. The possibility of the presence of a secondary process occurring within the oxide film acting in a manner to affect its ability to quench the oxidation rate will be considered below.

The A and D capsule systems contained the same concentrations of iron(II) chloride except that the inner metal surface of the latter capsule system was rinsed several times with FeCl_2 in an attempt to remove any manganese present as a 0.57-weight-percent impurity (see Table 1) from the surface phases. The forward metathetical reaction



has a standard free energy of reaction ΔG° , based on the respective standard oxidation potentials of the metals, of -34.0 kcal/mole. At equilibrium (25°C), the ratio

$$\frac{[\text{Mn}^{2+}]}{[\text{Fe}^{2+}]} = 10^{25} \quad (11)$$

has been calculated for reaction (10).

The appearance of the second peak, attributed to an alternate oxidation process, in Fig. 3 for set D, may signal the effect that the reaccumulation of manganese, concurrent with the oxidation of the wall metal, may have on the oxidation rate. In contrast, the unselective erosion of the iron surface in those systems (sets B and C) where iron(II) chloride was produced in situ by the action of hydrochloric acid did not yield such deviant results. Evans (22) postulates that minor alloying constituents having a much greater affinity for oxygen (in this case, manganese) than that of the matrix metal would be preferentially oxidized and concentrate as an intermediate layer at the metal/oxide interface. Evidence of a possible separate MnO-enriched phase in the surface oxide film has been obtained by x-ray diffraction analysis (9). The presence of the second oxidation rate peak for the D system and the long decay to the plateau region for the A system may be indicative of the role of manganese in the creation of vacancies in the oxidation zone that could coalesce, according to the suggestion by Douglass (13), into cavities and contribute to film porosity.

The reduced peak oxidation rate for set D compared to set A is attributed to the formation of iron oxides on the metal substrates consequent to their being washed by FeCl_2 solution in air. This is supported by the observation that reduced peak oxidation rates have been obtained in all cases where iron specimens possessed a preformed, though invisible (to the eye), surface oxide film. For example, the iron specimens used in this investigation had been permitted to age 2 years in a desiccator following their hydrogen and vacuum anneal and yielded peak oxidation rates that were 12% lower than the corresponding value for nonaged specimens. Their plateau region oxidation rates remained unaltered, however. No further studies have been made on the possible relation between the manganese content of the iron and its oxidative behavior at elevated temperatures.

Variations in the chemical treatment of the iron surfaces for the A, B, C, and D systems prior to oxidation have altered the values of the adjustable parameters a and b in the log term of Eq. (7), while the value of k' has maintained a constant value, Table 4. It is apparent that the characteristic oxidative rate behavior of iron is a function of k' and is located in the plateau region where a steady-state condition is maintained on a surface covered with an oxide film. The numerical value of k used in Eq. (3) represents an approximation obtained by disregarding other less possible rate processes. Thus, it would be of interest to compare the oxidative behavior of iron in the plateau region with the results of other investigations performed under similar conditions.

Potter and Mann (5, 6, 19) studied the chloride-induced oxidation of iron at elevated temperatures by placing their iron specimens in an autoclave and measuring the growth of a preformed oxide film. In this method, the only escape path for the hydrogen formed as a reaction end product was through the oxide film. They found (6) that a linear growth law could be obtained only if a low-hydrogen-overvoltage cathode, e.g., a film of nickel, were deposited at the oxide/solution region. Without this artifice to withdraw the solvated hydrogen ions from the region where the metal substrate, oxide film, and the electrolyte have a common interface, a very erratic oxidation resulted that was characterized by

spalling and exfoliation of the oxide film. Their rates of oxidation or linear growth law slopes depended on the mass of nickel deposited per unit area. For their experimental results, a linear film growth law can be obtained that is proportional to the cube root of the weight of metallic nickel, in milligrams per sq cm, that is deposited at the oxide/solution interface; e.g.

$$W = k'' (\text{Ni})^{1/3} t \quad (12)$$

$$k'' = (3.85 \pm 0.15) \times 10^4 \frac{\text{mg Fe}}{\text{dm}^2\text{-mo}} \times \frac{1}{\text{mole}} \left(\frac{\text{cm}^2}{\text{mg Ni}} \right)^{1/3}$$

Differentiating Eq. (12) with respect to t to obtain the rate,

$$\frac{dW}{dt} = k'' (\text{Ni})^{1/3}, \quad (13)$$

and making the assumption that k'' of Eq. (13) is also a function of the electrolyte concentration,

$$k'' = k''' [\text{Fe}^{2+}]^{1/2} [\text{Cl}^-]^{1/2}, \quad (14)$$

Eq. (13) becomes

$$\frac{dW}{dt} = k''' (\text{Ni})^{1/3} [\text{Fe}^{2+}]^{1/2} [\text{Cl}^-]^{1/2}, \quad (15)$$

where

$$k''' = (2.61 \pm 0.11) \times 10^5 \frac{\text{mg Fe}}{\text{dm}^2\text{-mo}} \times \frac{1}{\text{mole}} \left(\frac{\text{cm}^2}{\text{mg Ni}} \right)^{1/3}$$

If $k''' (\text{Ni})^{1/3}$ is considered to be equivalent to the kinetic rate constant k' , Eq. (15) is identical form with that of the plateau rate equation for Eq. (3); e.g.,

$$\frac{dW}{dt} = k' [\text{Fe}^{2+}]^{1/2} [\text{Cl}^-]^{1/2}, \quad (3)$$

where the value of k' obtained in this investigation (Eq. (7) and Table 4) is 8.14×10^5 mg Fe l/dm²-mo-mole, and the ratio

$$\frac{k'}{k'''} = 3.1 (\text{Ni})^{1/3} \left(\frac{\text{mg Ni}}{\text{cm}^2} \right)^{1/3}. \quad (16)$$

Potter and Mann's oxidation was of iron specimens possessing a preformed oxide film and their data precluded the presence in Eq. (12) of a log term descriptive of an early film growth proceeding by a pore filling-pore generating mechanism such as had been obtained in Eq. (7).

Habashi (23) has examined oxidation reactions undergone by several metals that were characterized by the single fact that no insoluble reaction end product was formed at the metal/solution interface to hinder the heterogeneous phase reaction. Postulating an

electrochemical mechanism for the oxidation process with a slow or rate-determining step described as the diffusive transport across the Nernst boundary layer by a depolarizer to the cathodic region and a complexing agent toward the anodic region, Habashi obtained the following rate equation to fit the data:

$$(\text{RATE}) = A \frac{k_1 [\text{C}] k_2 [\text{D}]}{k_1 [\text{C}] + k_2 [\text{D}]}, \quad (17)$$

where

A = total surface area in contact with the electrolyte,

k_1, k_2 = kinetic rate constants,

$[\text{C}], [\text{D}]$ = concentration of reagents whose diffusive transport across the respective anodic and cathodic region Nernst layers determine the reaction rate.

When $k_1 [\text{C}] = k_2 [\text{D}]$, Eq. (17) may be written as

$$(\text{RATE}) = 1/2 (k_1 k_2)^{1/2} A [\text{C}]^{1/2} [\text{D}]^{1/2} \quad (18)$$

or

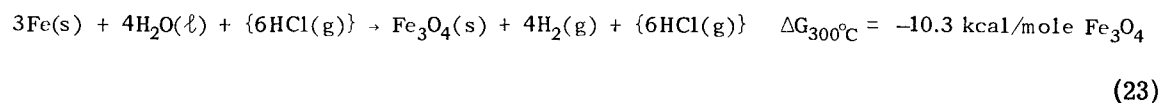
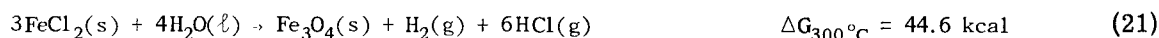
$$(\text{RATE}) = k^{IV} [\text{C}]^{1/2} [\text{D}]^{1/2} \quad (19)$$

which is identical form with Eq. (3) found in this investigation and where the metal substrate contained a tight adherent film of Fe_3O_4 , shown in Fig. 6. The validity of Eq. (17), proposed by Habashi, in the form of

$$\left(\frac{dW}{dt}\right) = \frac{k_1 [\text{Fe}^{2+}] k_2 [\text{Cl}^-]}{k_1 [\text{Fe}^{2+}] + k_2 [\text{Cl}^-]} \quad (20)$$

is undergoing further investigation.

The thermodynamics of the oxidation of iron at 300°C was calculated from Kubaschewski and Evan's data (24):



where the subscripts s, l, and g represent the solid, liquid, and gaseous states, respectively. The summation of Eq. (21) and (22) yields Eq. (23), which is equivalent to Eq. (1) proposed earlier as the fundamental oxidation reaction. It may be postulated that the function of the oxidizing solution would be to alter the rate of reaction; it does not enter into the final reaction product. The oxidation of FeCl_2 to the experimentally determined solid surface phase, Fe_3O_4 (in Eq. (21)), represents a very unfavorable thermodynamic reaction unless the reaction product, HCl , is considered to react further with additional Fe as in Eq. (22). The free energy of reaction in Eq. (23) corresponds with that given in the literature (Ref. 25) so that a cyclic process is postulated and is expressed symbolically by the inclusion of $\{6\text{HCl}_{(g)}\}$ on both sides of Eq. (23). It is apparent in this analysis that the chloride ion, as HCl in this case, functions as a catalyst to the oxidation reaction.

The rate of precipitation of iron(II) from solution to the oxide surface, and hence its replenishment from the metal/solution interface by the continued oxidation of elemental iron, would be expected to be a function of the iron(II) concentration. It is not clear at present whether a rate-controlling step in the overall reaction would be the depolarization at the cathodic regions by, or the reduction of, the solvated proton. The concentration of this ion would be a function of the iron(II) concentration.

Silverman and Dodson (26) investigated the homogeneous solution behavior of anions in the redox reaction between iron(II)/iron(III). They proposed that the rate of electron transfer was accelerated by anions, such as chloride and hydroxide, by forming an activated binuclear bridge complex intermediate. The catalytic activity of the hydroxyl ion was several orders of magnitude greater than that of the chloride ion. Simonova and Rotinyan (27) extended this concept to the heterogeneous reaction at the iron/solution interface. When water and the hydroxyl ion participate in the activated intermediate binuclear bridge complex between the metal and its solvated iron(II) ion, the low-solubility oxidation products that are ultimately formed are precipitated in the immediate area of the anodic site, thus quenching the reaction. The presence of chloride ions in sufficient concentration leads to a condition where the soluble iron(II) chloride diffusing away from the anodic region is deposited as basic iron compounds by hydroxyl ions diffusing toward the anodic region. The released chloride ions are free to return to the anodic sites. Hydroxyl ions are continually being removed from solution and prevented from reaching an anodic site by reacting with the outwardly diffusing iron salts.

Eventually, chloride ions concentrate at the metal/oxide-metal/solution common interface to the exclusion of the hydroxyl ion, which paradoxically displays the greatest catalytic activity. The porous oxide film synergistically aids in this process by confining the countercurrent ion migrations as pore-localized phenomena so that the oxide film may be ultimately regarded as an ionic sieve. The discriminating action of such a sieve does not depend on its pore sizes nor on the sizes of the ions under discussion but on the abilities of anions, such as the chloride ion, to diffuse toward anodic regions at the metal/oxide-metal/solution interface without being precipitated, chemically altered, or otherwise diminished in concentration.

ACKNOWLEDGMENTS

The author thanks the following colleagues: Dr. Mortimer Bloom, with whom he had many thought-provoking discussions, Mr. Leo Goldenberg, who performed the oxidations with iron(II) sulfate and distilled water, Mr. Elliott Osgood, whose aid and counsel contributed to this research effort, and Dr. Robert Jones, for preparing the electron photomicrograph.

REFERENCES

1. Foley, R. T., Goldberg, D., and Carlston, R. C., Final Report to the Office of Naval Research, Part I, AD 686, 481, Washington, D. C., Oct. 1968
2. Foley, R. T., Final Report to the Office of Naval Research, Part II, AD 686, 518, Washington, D. C., Mar. 1969
3. Bloom, M. C., "A Survey of Steel Corrosion Mechanisms Pertinent to Steam Power Generation," 21st Annual Water Conference, Engineers' Society of Western Pennsylvania, Oct. 21, 1960
4. Slater, I. G., and Parr, N. L., Proc. Inst. Mech. Eng. 160:341 (1949)
5. Potter, E. C., and Mann, G. M. W., Chem. Ind. (London) 1963: 1768 (1963)
6. Potter, E. C., and Mann, G. M. W., Brit. Corrosion J. 1:26 (1965)
7. Bloom, M. C., and Krulfeld, M., J. Electrochem. Soc. 104:264 (1957)
8. Fraser, W. A., and Bloom, M. C., Corrosion 18:163t (1962)
9. Scheiman, M. A., in preparation
10. Jones, R., personal communication
11. Evans, U. R., Chapter 20 in "The Corrosion and Oxidation of Metals," London: Edward Arnold London, 1960
12. Harrison, P. L., J. Electrochem. Soc. 112:235 (1965)
13. Douglass, D. L., Oxidation of Metals 1:127 (1969)
14. Evans, U. R., "The Corrosion and Oxidation of Metals," London: Edward Arnold, pp. 29, 827-829, 1960
15. Tomashov, N. D., "Theory of Corrosion and Protection of Metals," B. H. Tytell, I. Gold, and H. S. Preiser, translators, New York: Macmillan, pp. 45-47, 1966
16. Wyn Roberts, M., Trans. Faraday Soc. 57:99 (1961)
17. Tomashov, N. D., "Theory of Corrosion and Protection of Metals," B. H. Tytell, I. Gold, and H. S. Preiser, translators, New York: Macmillan, pp. 87-90, 1966
18. Tomashov, N. D., "Theory of Corrosion and Protection of Metals," B. H. Tytell, I. Gold, and H. S. Preiser, translators, New York: Macmillan, p. 91, 1966
19. Mann, G. M. W., Chem. Ind. (London) 1964: 1584 (1964)
20. Castle, J. E., and Masterson, H. G., Corrosion Sci. 6:93 (1966)
21. Bloom, M. C., Newport, G. N., and Fraser, W. A., J. Electrochem. Soc. 111:1343 (1964)

22. Evans, U.R., "The Corrosion and Oxidation of Metals," London: Edward Arnold, Chapter II and p. 836, 1960
23. Habashi, F., J. Chem. Ed. 42:318 (1965)
24. Kubaschewski, O., and Evans, E.Ll., Chapter IV in "Metallurgical Thermochemistry," 3rd ed., New York: Pergamon, 1958
25. Linnenbom, V.J., J. Electrochem. Soc. 105:322 (1958)
26. Silverman, J., and Dodson, R.W., J. Phys. Chem. 56:846 (1952)
27. Simonova, M.V., and Rotinyan, A.L., Russ. Chem. Rev. 34:318 (1965)